# Computation of Air Entrainment into a Mixing Pipe: An Experimental and Numerical Analysis

*Dipti Prasad Mishra*[*]*, Subhash Chandra Paramanik*
*Birla Institute of Technology, Mesra, Ranchi, India*
**diptimishraster@gmail.com*

ABSTRACT

*Computations of entrainment of air into a pipe were performed by placing an air jet at the bottom of the pipe. An experiment was performed with cylindrical mixing pipe having different diameter, length and jet location. A flow meter was used to measure the flow through the nozzle and velocity at the mixing pipe exit was measured by anemometer. CFD analyses were performed using Ansys-Fluent 16 to match the experimental results for exit velocity and amount of air sucked into the pipe. Further numerical investigations were performed for a mixing pipe with hot jet to estimate the amount of air entrained as a function pipe diameter, pipe length, nozzle protrusion and pipe shape. It was found from the numerical simulations there exists an optimum pipe length and nozzle protrusion for highest entrainment of air. Also a particular frustum shaped pipe could suck highest air compared to cylindrical shaped pipe.*

**Keywords:** A*ir Jet, Mixing Pipe, Protrusion, Pipe Length, Pipe Shape*

## Introduction

The practical utilisation of air entrainment into the pipe is found in the naval ships where the hot combustion products could be cooled by mixing with the surrounding air. The funnel of naval ships is used to eject the combustion products of the gas turbine to the surrounding atmosphere. The exhaust pipe from the turbine outlet protrudes into the funnel. The high velocity combustion products at the pipe exit are hot which may be cooled by mixing with the surrounding air sucked from the surrounding. The pressure inside the funnel is low due the high speed jet, as result it sucks air from the surrounding domain through the bottom opening funnel. The two streams of

ISSN 1823-5514, eISSN2550-164X
Received for review: 2018-07-08
Accepted for publication: 2019-04-08
Published: 2019-08-31
© 2018 Faculty of Mechanical Engineering,
Universiti Teknologi MARA (UiTM), Malaysia.

gases mixed inside the funnel and finally expelled to the surrounding atmosphere. By the time it is reached at top of the funnel the combustion products cooled down to low temperature. It is very much essential in war ship where the enemy ship may spot the war ship at the mid ocean from the infrared (IR) signals of hot combustion products and could have targeted it which is absolutely not desired. The funnel here served as a mixing pipe in the present investigation. The air is allowed to entrain into the pipe at the bottom of a mixing because of low pressure of the jet. The temperature of combustion products at the mixing pipe exit depends upon the amount of air entrained into the mixing pipe. Therefore the motivation of the research is to design the mixing pipe to obtain the highest air suction using appropriate computational fluid dynamics (CFD) methodology.

Cramers et al. [1] concluded from the experimental investigations the gas entrainment into a liquid jet ejector increased with density of the gas. They have also revealed that the suction rate was increased by placing a whirling body into the nozzle. Chan et al. [2] performed sequence of experiments by using annular counter flow of combustion products to study the effects of the jet diffusion flame and concluded that for lesser outer tube diameter the blow out is good and mixing improvement was found to be better. Jifei et al. [3] developed the relation between the suction rate performance with $R_1$ (mixing tube length/mixing tube diameter) and suction rate performance with $R_2$ (horizontal length inlet of mixing pipe from the nozzle/diameter of water nozzle) for jet aerator. They concluded that $R_1$ and $R_2$ have an optimum value for highest suction rate.

Mishra and Dash [4] predicted the mass suction rate, exit temperature and entrance length of sucking funnel using CFD analysis. General correlations were developed for exit temperature and mass suction rate in terms of the non-dimensional quantities. Mishra et al. [5, 6, 7] performed a series of numerical and experimental investigations to compute the maximum air entrainment of a closed bottom laterally opening mixing pipe (funnel) for different nozzle and pipe configurations. They have developed a number of correlations to compute the air suction rate, funnel exit temperature and entrance length for a sucking pipe.

Barik et al. [8] performed investigation experimental and numerical for both isothermal jet and hot jet. He concluded that the mass ingress of air depends on the nozzle protrusion and louvers opening area. They have also developed many correlations for the range of Reynolds number $3525 \leq Re \leq 8000$ to compute the air entrainment and fluid exit temperature. The mass suction of air for bottom opening pipe has been investigated numerically by Mishra et al. [9]. They found that there exist optimum pipe diameter, shape, length and nozzle location for maximum air entrainment. They have also concluded for a simple pipe the entrance length much longer compare to the

cylindrical sucking pipe for same Reynolds number and uniform inlet velocity.

Optimum overlap of an Infrared supression (IRS) device was computed numerically and experimentally by Barik et al. [10]. They concluded that the entrainment is reduced by 15.94% when the overlap length changed from 0 to 1.6. He also pointed out the circular jet entrain less than non-circular jet. Sahu and Mishra [11, 12, 13] performed CFD analysis to compute the entrainment into a mixing pipe having open and closed entrance by using single and multiple nozzles. They have concluded that the entrainment rate increases by using multiple nozzles instead of single one. Mohd Noor et al. [14] predicted output torque, brake power, brake specific fuel consumption and exhaust gas temperature of a marine diesel engine using artificial nueral network (ANN). The predicted data set of the model was compared with the measured experiment data. The results showed that the ANN model have a good agreement with the experimental data. The prediction error in ANN model low compared to mathematical model.

In the present investigations, a laboratory scaled experiment has been performed to compute the entrainment rate of air into a pipe for different pipe and nozzle configuration for an isothermal jet. CFD analyses have been carried out to match the experimental results with numerical results. Further computations have been done for hot jet (40 ºC to 80 ºC) by varying the mixing pipe shape, size and location of nozzle to compute the maximum entrainment rate of air into a open ended pipe which is the main objective of the present work.

## Experimental Setup

Schematic diagram of experimental set up has been shown in Figure 1(i) where as Figure 2 shows the snap view of actual set up. A cylindrical acrylic pipe which is opened at both ends i.e. top and bottom. The mixing pipe diameters ($D_f$) are 0.047, 0.072, 0.095 and 0.115 meter and the length of the mixing pipes ($H_f$) 0.6096, 0.9144 and 1.2192 metre have been considered for present experiment. An iron stand is used to hold the pipes vertically (shown in Figure 2). A nozzle is placed at the bottom centre of the pipe to provide a jet of air into the pipe. A compressor is used to supply high pressure air to air storage tank from where it is supplied to the nozzle and a control valve is used to control the flow. A flow meter is connected before the nozzle to mesure the air flow throgh the nozzle. By using the flowmeter the volume flow rate of air is muasured and after mulplying the density of air the mass flow rate through the nozzle is computed.A thin thread is fixed at the exit of the mixing pipe/funnel. This thread is marked with ink at regular interval. The flow velocity of air is measured at the marking points using hotwire

anemometer. The area of a particular strip (say $A_2$) is determined using formula $\int 2\pi r dr$ as shown in the Figure 1(ii).Then the air velocity is multiplied with the density of air and that strip of area ($A_2$), the mass flow rate for that strip is computed.Similar procedure is adopted to compute the mass flow rate of other strips ($A_1$, $A_3$ etc.). Then the total mass flow rate is computed by adding all these mass flow rates,which is given by $\int V\rho 2\pi r dr$,where V is the velocity of air, r is the radial distance and ρ density of air. The rate of air entrainment through the mixing pipe bottom is obtained from the difference of mass flow rate at the mixing pipe outlet and nozzle inlet. By varying the length, diameter and nozzle protrusioninto the pipe the rate of entrainment into the pipe is computed.

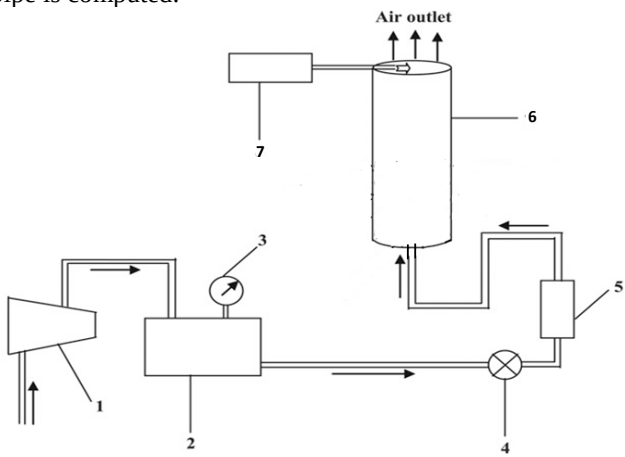


1. Air compressor 2. Compressed air tank 3. Pressure gauge 4. Control valve
5. Flow meter 6. Cylindrical funnel 7. Anemometer

Figure 1: (i) Experimental Set up: A Schematic view

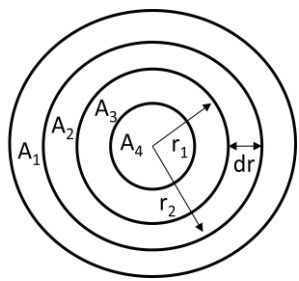


Figure 1: (ii) Schematic diagram mixing pipe exit area

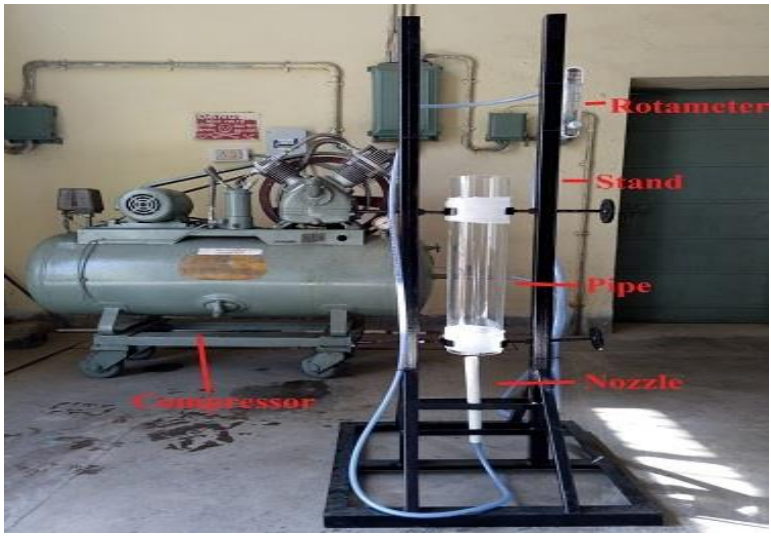


Figure 2: Snap view of experimental set up

## Numerical Procedure

Two dimensional discretised governing equations were solved by commercial software Fluent 16 by applying appropriate boundary conditions. To improve accuracy second order scheme was used after getting converged solution from first order upwind scheme. Figure 3 shows the boundary conditions applied to the computational domain. The problem is considered to be axi-symmetric. A bigger computational domain is taken, which is six times the diameter of the pipe and three times the length of the pipe and pressure outlet boundary condition was applied at all sides of the domain. The value of pressure has been taken to be zero gauge pressure in numerical simulation, because for incompressible flow absolute prssure is not very important.The velocity will be determined at pressure outlet boundary from local pressure field in order to satisfy the continuity equation where as other scalar varibles are computed from zero gradient condition [15]. The pipe and nozzle walls are given no-slip boundary conditions where as temperature and velocity inlet condition has been given at outlet of the nozzle. An uniform velocity profile has been imposed at the nozzle exit. The Reynolds number based on nozzle diameter is maintained constant at 2800. Two dimensional incompressible Navier-Stokes equations and energy equation were solved along with a two equation based k-ε turbulence model.

Table 1: Variation of suction rate with grid number

| Number of grids | $\dot{m}_{suction}$ (kg/s) |
|---|---|
| 2005 | 0.0014 |
| 4087 | 0.00183 |
| 6213 | 0.00216 |
| 8153 | 0.00242 |
| 10329 | 0.00253 |
| 12028 | 0.00262 |
| 14051 | 0.00265 |

A grid density test has been conducted before proceeding for the numerical computations. It is noticed by increasing the grid number the air entrainment into the pipe increases. Initially course meshes is considered (corresponding to grid number 2005) and afterwards meshes have been refined so that the grid numbers is increased up to 14051. It has been observed from the investigation beyond the grid number 12028; the air entrainment into the pipe does not vary any more. So this cell size is chosen for all the parametric investigations.

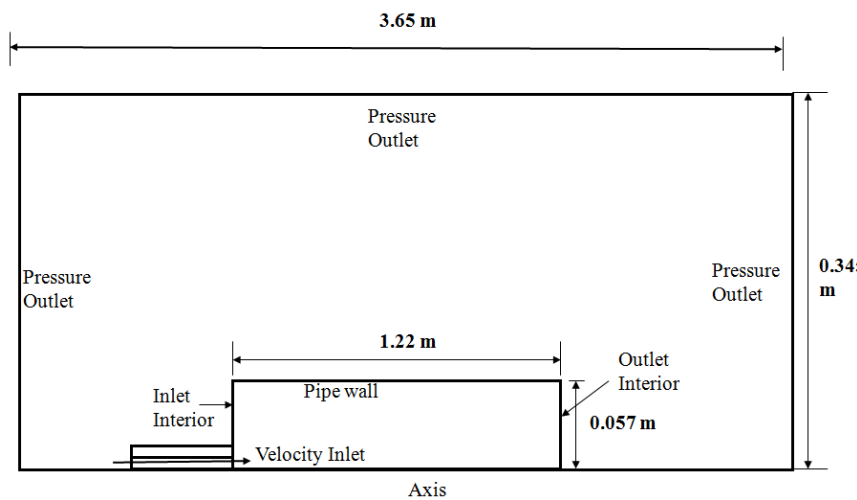


Figure 3: Computational domain showing the boundary conditions

## Results And Discussions

### Effect of mixing pipe diameters on entrainment rate

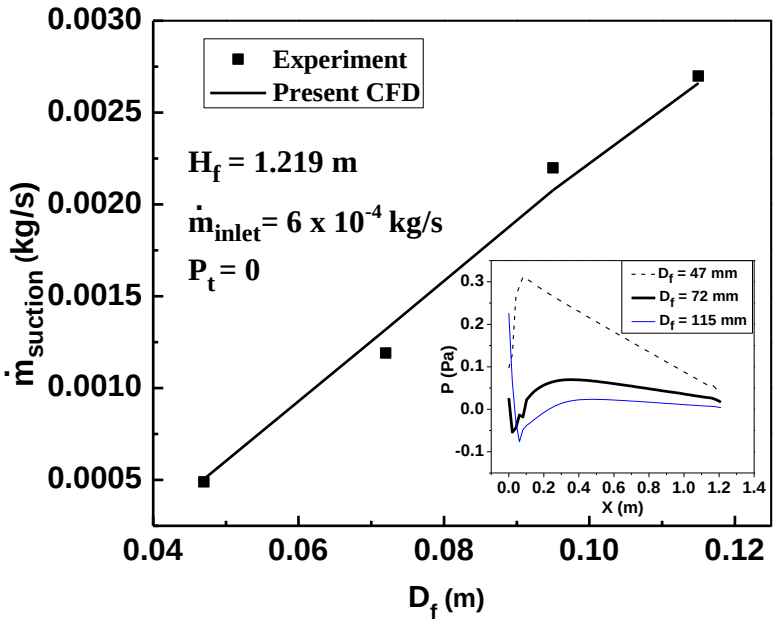


Figure 4: Effect of pipe diameter variation on air entrainment

Experimental and computational (CFD) analyses have been performed by the changing the mixing pipe diameter 47, 72, 95 and 120 mm. The paramters nozzle flow rate ($\dot{m}_{inlet}$), length of mixing pipe ($H_f$) and nozzle protrusion ($P_t$) are kept constant at 6 x $10^{-4}$ kg/s, 1.219 m and 0 respectively (shown in Figure 4).The rate of entrainment ($\dot{m}_{suction}$) into the mixing pipe increases with the mixing pipe diameters. Figure 4 also shows the centreline pressure contour for three different mixing pipe dimeter (47 mm, 72 mm and 115 mm). It is clearly visualised from the plot the pressure is comparative high when the diameter of the pipe is low and as the diameter increases the centerline pressure decreases. This suggests as the diameter of the mixing pipe decreases the mass entrainment of air into the pipe deceases because of high viscous effect and low entrainment area of the fluid. When the pipe diameter increases the viscous effect decreases and also pressure inside the pipe falls (shown in Figure 4). When the pipe diameter increases the

entrainment areaalso increases, as a results more amount of air is rushed into the pipe. The CFD results match well with the experimental measurements.

### Effect of Nozzle Distance on Entrainment

Experimental and CFD analysis has been performed for isothermal jet for different nozzle distance ($P_t$) while mixing pipe length ($H_f$), its diameter ($D_f$), nozzle diameter ($D_n$) and nozzle flow rate ($\dot{m}_{inlet}$) are kept fixed. As shown in Figure 5 when the nozzle is kept away from the bottom is given negative value where as positive value is assigned when placed inside the pipe with reference to the entrance of the pipe. It can be visualised from plot as the nozzle protrudes into the pipe more and more the entrainment rate increases and reaches a maximum value corresponding to 2 cm protrusion after that it falls (both experimentally and numerically). This suggests for the present situation the optimum nozzle protrusion is 2 cm into the pipe. Pipe designer always look for the optimum distance of the nozzle for placement to suck

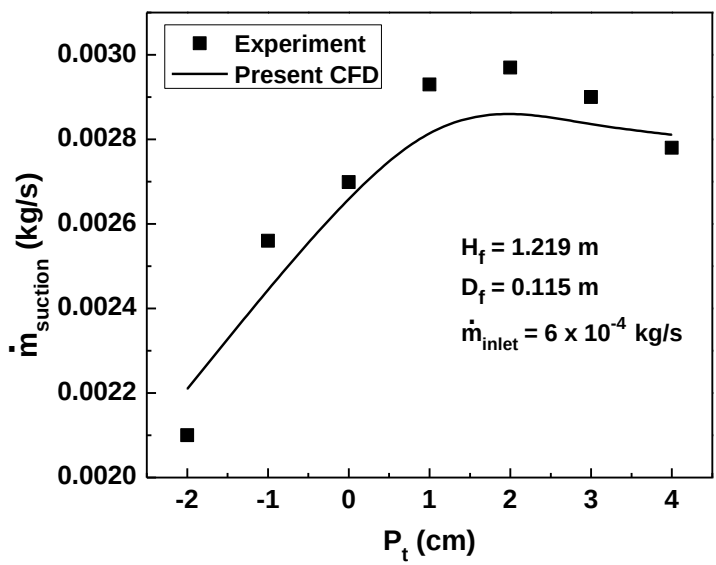


Figure 5: Entrainment rate variation as a function of nozzle protrusion

maximum amount of air into the pipe. The low pressure zone created inside the mixing pipe is a prime factor for air to be sucked into the mixing pipe. It is seen from the plot the maximum difference between the experimental

results and computational results is found to be within 5% considering experiment as the baseline case.

## Variation of suction rate as a function of pipe length

Figure 6 shows the variation of entrainment rate with pipe lengthfor a nozzle flow rate ($\dot{m}_{inlet}$) of 6 x $10^{-4}$ kg/s. In the present investigation nozzle protrusion is set at zero level ($P_t$) and the mixing pipe diameter ($D_f$) kept constant at 0.115 m. It can be seen from the plot by rising the length of the pipe the air entrainment decreases. It indicates by increasing the pipe length the viscous resistance rises, so entrainment into the pipe decreases. The experiment seems to have a good agreement with numerical results.

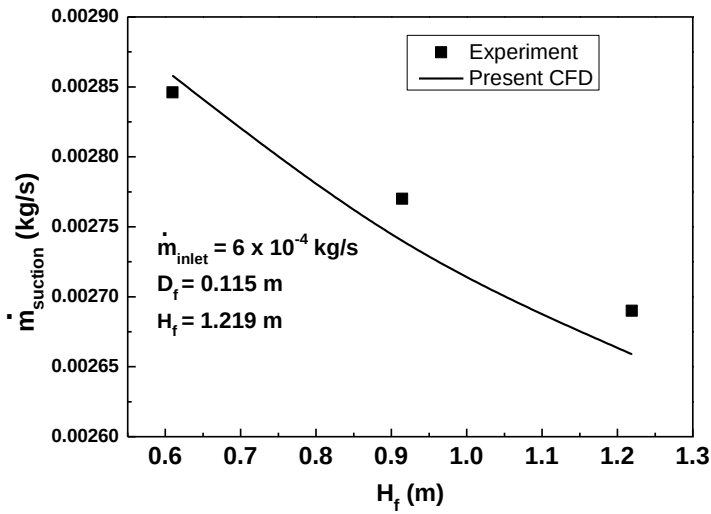


Figure 6: Variation of entrainment rate as a function of pipe length

## Velocity profile at the mixing pipe exit

Figure 7 and 8 show the experimental and computational axial velocities ($V_x$) at different radial distances (r) on the exit surface of the mixing pipe for two different mixing pipe length. It can be seen from the figure that there is a reasonably good match between the experimentally and CFD velocity profile. Near at the centre of the mixing pipe, there is a slight degree of mismatch between the computational velocity and the measured (experimental) velocity profile. The two equation based k-ε model has been used for turbulent modelling to compute velocity and the centreline velocity may be dropped because the k-ε model is over diffusive and tries to create more mixing of

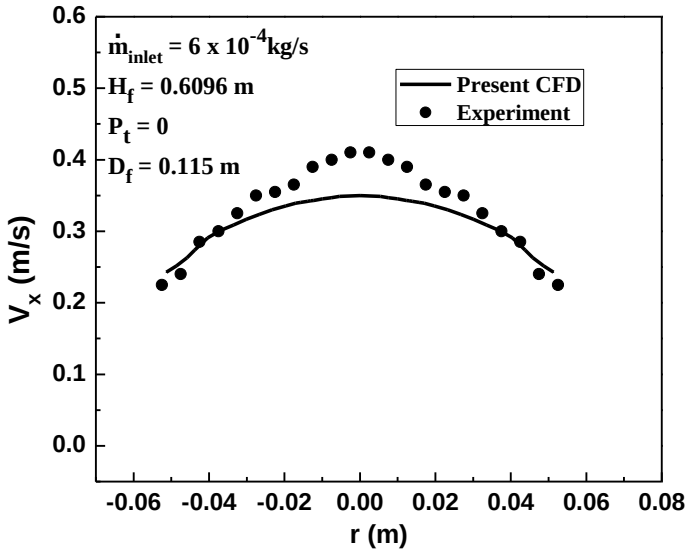


Figure 7: Pipe exit axial velocity profile: A comparison between experimental and CFD Results (Mixing Pipe length is 0.609 m)

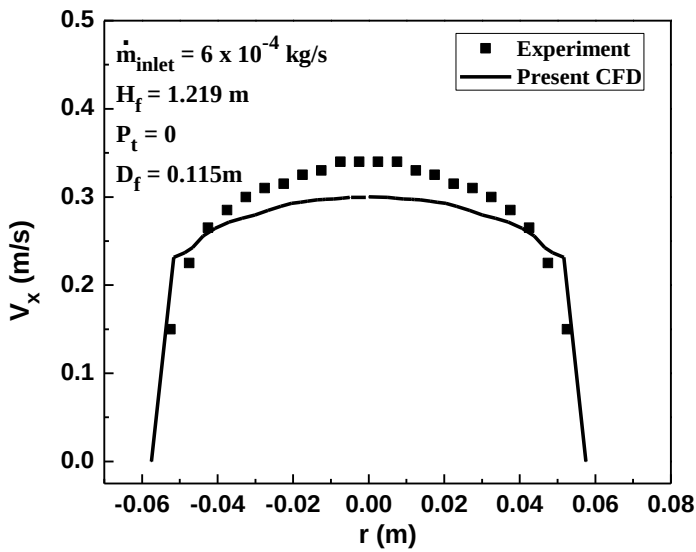


Figure 8: Axial velocity at the top of the mixing pipe: A comparison between Experimental and CFD Results (Mixing Pipe length is 1.219m)

momentum, which is seen clearly in Figure 7 and 8. The velocity profile in Figure 7 is steep because the flow is not fully developed due to small length of the pipe and as the length of the pipe increases the flow slowly developing and the velocity profile is flat (Figure 8). The maximum difference between experimental and CFD obtained velocity profile is found to be 15% and it is seen near the centre of pipe. The k-ε turbulent model imposed to compute the the velocity is too diffusive which may not able to compute the velocity of a sucking pipe at the centre accurately. However the computted velocity profile away from the centre matches well with the experment value.

### Effect of mixing pipe diameter on entrainment for hot jet

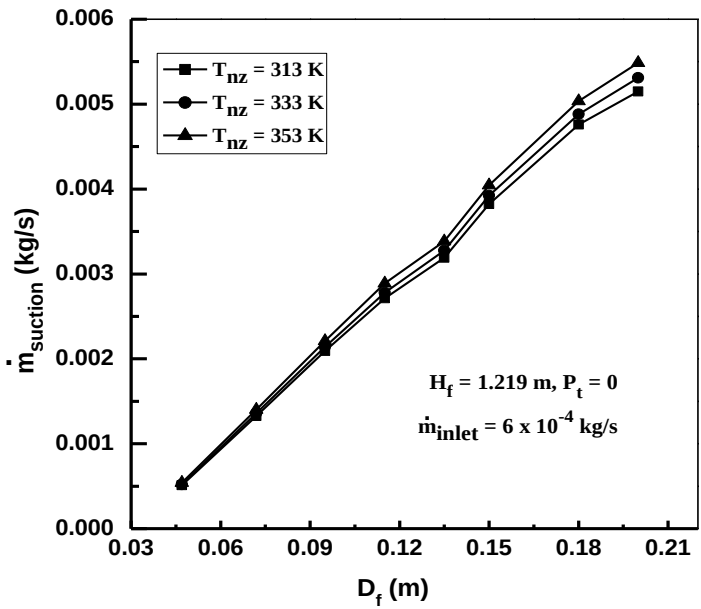


Figure 9: Entrainment rate as a function pipe diameter

Further CFD simulations have been performed for hot jet at different inlet temperature ($T_{nz}$) and diameter of mixing pipe ($D_f$) where the air flow rate throgh the nozzle ($\dot{m}_{inlet}$) and other operating parameters have been kept constant as shown in Figure 9. It may be visualised from the plot as the diameter of mixing pipe increases the mass suction of air ($\dot{m}_{suction}$) increases because of increase in opening area of the mixing pipe.It is also observed from the plot at higher jet temperature more air is sucked into the mixing due to the buoyancy effect.

## General view of suction process

The velocity vector plot of the entire domain is shown in Figure 10. The numerical simulation has been performed for the mixing pipe length ($H_f$), diameter of the mixing pipe ($D_f$) and diameter of the nozzle ($D_n$) 1.219 m, 0.115 m and 0.019 m respectively. The domain length ($H_{cd}$) and diameter ($D_{cd}$) is taken as 3.657 m and 0.69 m respectively. It is seen that due to the high velocity central jet the air enters the mixing pipe from the bottom and leaves at the top. The central jet is dragged the flow axially in upward direction and discharged at the top. The low pressure is created by the central jet enables to suck the air from the surroundings and also drives the sucked air towards the top due to its own kinetic energy.

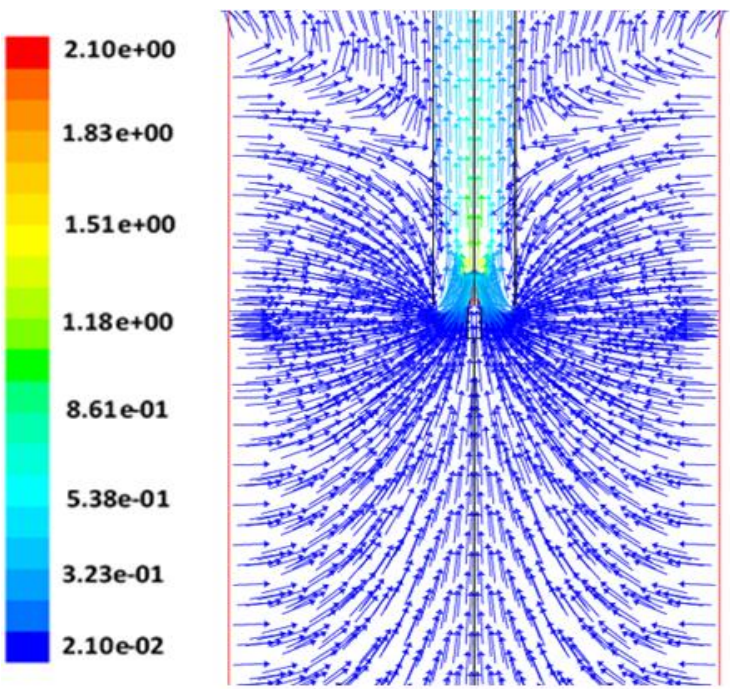


**$D_f$ = 0.115 m, $H_f$ = 1.219 m, $\dot{m}_{inlet}$ = 6 x $10^{-4}$ kg/s**
**$D_n$ = 0.019 m, $H_{cd}$ x $D_{cd}$ = 3.657m x 0.69 m**

Figure 10: Velocity vector in the computational domain, showing air entrainment at the bottom of the pipe and dragged by central jet

### Effect of nozzle distance on mass suction for hot jet

CFD analysis has been performed for hot jet for different nozzle protrusion ($P_t$) while the pipe length ($H_f$), diameter ($D_f$), nozzle diameter ($D_n$) and nozzle flow rate ($\dot{m}_{inlet}$) have been maintained constant. Nozzle fluid temperature ($T_{nz}$) is varied in the range 313 K to 353 K. Figure 11 shows as the nozzle advances towards the bottom of the pipe the entrainment rate of air increases and it is seen from the plot the placement of nozzle at a distance of 1 cm into the pipe the entrainment is found to be maximum. It is also noticed from the plot when the nozzle protrudes more into the mixing pipe again the entrainment falls, suggesting optimum distance of nozzle for highest entrainment of air and in the present case it is found to be at a distance of 1 cm from the entrance of the pipe. In isothermal jet case, shown in Figure 5, the air jet is at the surrounding temperature which sucks the air into the mixing pipe due to low pressure created by the high velocity jet inside the pipe. However, in hot jet case shown in Figure 11 additional driving force acts on the fluid due to buoyancy. As a result, more amount of fluid is sucked into the mixing pipe and the optimum protrusion is comparatively less for hot jet than that of isothermal jet.

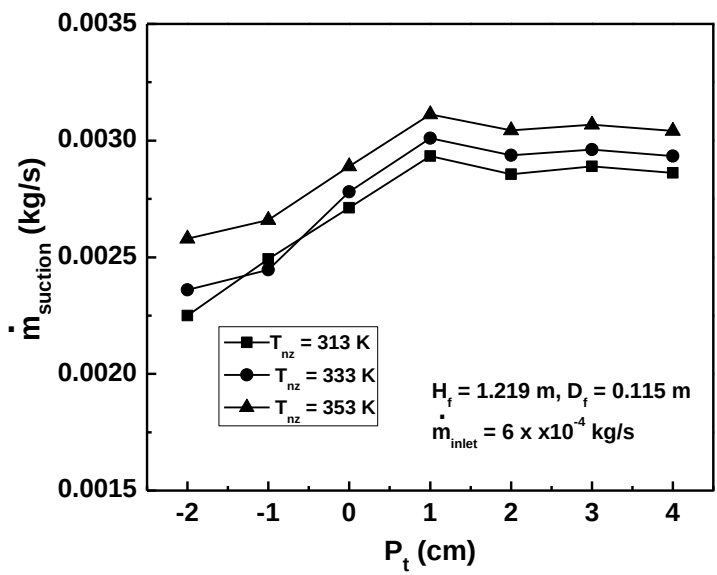


Figure 11: Variation of entrainment rate as a function of nozzle protrusion

### Effect of mixing pipe length on entrainment rate for hot jet

Figure 12 shows air entrainment rate with the length of the mixing pipe for a flow rate through the nozzle ($\dot{m}_{inlet}$) 6 x $10^{-4}$ kg/s at different nozzle fluid temperature ($T_{nz}$). In the present CFD investigation the diameter of mixing pipe and nozzle protrusion were kept constant. It has been found that with increase in pipe length the entrainment into the pipe length ($H_f$) increases from 0.3048 m to 0.6096 m and then decreases with further increasing the mixing pipe length. The high velocity jet creates a low pressure inside the mixing pipe a little away from the nozzle tip. When the length of the pipe increases more fluid from the surroundings is entrained into the pipe due to suction effect of the jet. However, as pipe length increases more than a certain limit the entrainment falls due to the viscous effect of the flow. So, in the present case an optimum length of the pipe is found to be at 0.6096 m for maximum entrainment.

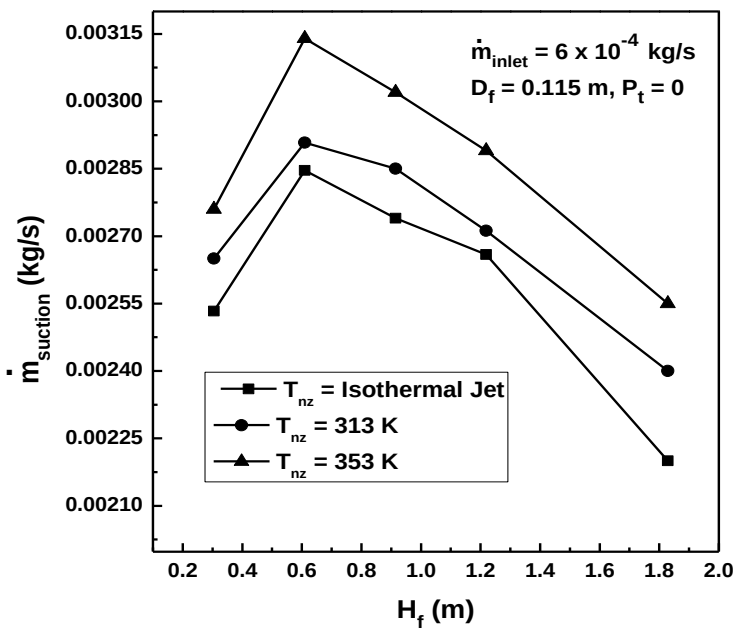


Figure 12: Air entrainment into the pipe at different pipe length

## Effect of pipe shape on air entrainment

Mixing pipe shape has been changed from cylindrical to frustum shape while keeping the total volume and length to be constant for three nozzle fluid temperature ($T_{nz}$). The radius at the top of the frustum is considered to be $R_2$ where as bottom is considered $R_1$. The CFD analysis have been performed for frustum shape mixing pipe by varying the ratio of frustum radius top to bottom, $R_2/R_1$ while length of the frustum shape mixing pipe remain constant at 1.219 m. It is obtained from the numerical simulation (from Figure 13) at $R_2/R_1$ = 0.763 the air entrainment is maximum.The value of $R_2/R_1$ is more than 0.763, the mixing pipe opening area at the bottom decreases so air entrained into the frustum shaped pipe is less.If $R_2/R_1$ is less than 0.763, the exit area of the mixing pipe decreases and the viscous resistance to the flow increases, as a result the air entrainment falls. This indicates the frustum shaped mixing pipe having top diameter 0.76 times of bottom diameter has highest suction rate which is little higher than cylindrical mixing pipe ($R_2/R_1$ = 1) as shown in the Figure 13.

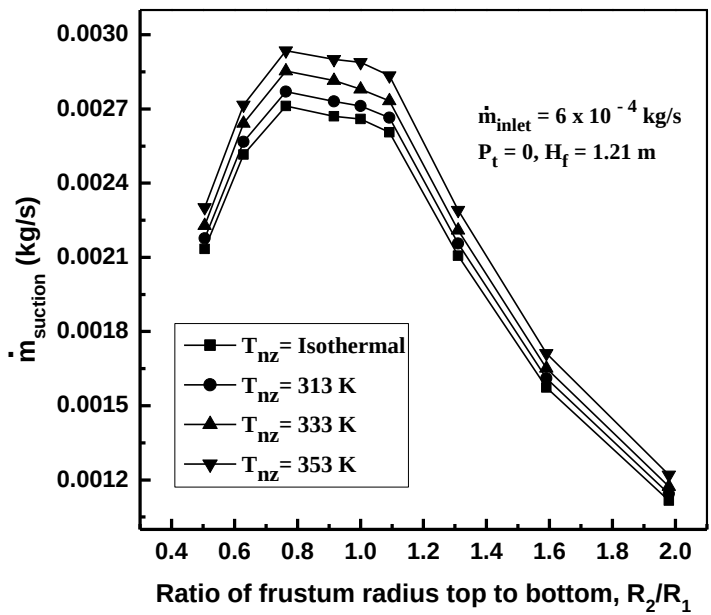


Figure 13: Variation of air entrainment for frustum shaped pipe, an optimum $R_2/R_1$ can be seen near 0.76

## Conclusions

Experimental and numerical computations have been performed by varying diameter, length, protrusion and different nozzle flow rate to compute the air entrainment into the pipe. The experimental investigation has been carried out using isothermal air jet while the computational analysis has been carried out both isothermal and hot jet. The following salient conclusions were derived from the present investigations:

- It was found from the investigation that as the diameter of the mixing pipe is increased the mass suction rate also increases both for isothermal jet and hot jet.
- For the present experimental and CFD investigation, it was found that an optimum nozzle protrusion is 2 cm for isothermal jet while for hot jet an optimum nozzle protrusion was found be at 1 cm from the CFD analysis.
- The highest air entrainment of air was found to be at 0.6 m length of the pipe for both isothermal as well as for hot jet and beyond this length the entrainment falls drastically.
- For a frustum shaped funnel with radius ratio of 0.763 (top to bottom) gives the highest mass ingress of air both for isothermal and hot jet.

## Acknowledgement

The authors are grateful to the Birla Institute of Technology, Mesra, for providing the financial support for experimental set up and the computational support (Fluent 16) to carry out the numerical analysis.

## Nomenclature

| | |
|---|---|
| ANN | artificial neural network |
| CFD | computational fluid dynamic |
| $D_{cd}$ | diameter of domain |
| $D_f$ | diameter of the mixing pipe |
| $D_n$ | nozzle diameter |
| $H_{cd}$ | length of the domain |
| $H_f$ | length of the mixing pipe |
| IRS | infrared suppression |
| $\dot{m}_{inlet}$ | air flow rate through the nozzle |
| $\dot{m}_{suction}$ | air entrainment into pipe |
| $P_t$ | nozzle protrusion |

| | |
|---|---|
| r | radial distance at mixing pipe exit |
| $R_1$ | bottom radius of the frustum |
| $R_2$ | top radius of the frustum |
| $T_{nz}$ | temperature of nozzle exit |
| V | velocity at mixing pipe exit |
| Vx | Axial velocity at different radial distance of pipe exit |
| ρ | density of air |

## References


[1] P.H.M.R.Cramers, "Dierendonck LLV. Beenackers AACM. Influence of the gas density on the gas entrainment rate and gas hold up in loop-venturi reactors,"*Chemical Engineering Science* 47,pp 2251–2256, 1992.

[2] S.M.S.Chan, S.Torii andT. Yano,"Enhancement of turbulent jet diffusion flame blowout limits by annular counter flow,"*International Journal of Energy Research* 25,pp 1091–1105, 2001.

[3] G. Jifei, G. Guowei, Z. Zilong andZ. Yalei Z,"CFD numerical simulation applied in the design of the jet aerator,"*Environmental Informatics Archives*, 3, pp 226-231, 2005.

[4] D.P. Mishra andS.K. Dash,"Prediction of entrance length and mass suction rate for a cylindrical. Funnel," *International Journals for Numerical method in fluids* 63,pp 681-700, 2010.

[5] D.P. Mishra, S.K. Dash andP.A. Kishan,"Isothermal Jet Suction through the lateral openings of a cylindrical funnel"*Journals of Ship Research* 54, pp 268-280, 2010.

[6] D.P. Mishra andS.K. Dash,"Numerical investigation of air suction through the louvers of a funnel,."*Computer and Fluids* 39,pp 1597-1608, 2010.

[7] D.P. Mishra andS.K. Dash,. "Maximum Air Suction into a Louvered Funnel Through Optimum Design,".*Journal of Ship Research* 56(1),pp 1-11, 2012.

[8] A.K. Barik, S.K. Dash, P. Patro andS. Mohapatra,"Experimental and numerical investigation of air entrainment into a louvred funnel,"*Applied Ocean Research* 48,pp 176-185, 2014.

[9] D.P. Mishra, M.K. Samantary andS.K. Dash,**"**Maximum air entrainment into a mixing pipe through optimum design,"*Ships and Offshore Structures* 9(6), pp 605–618, 2014.

[10] A.K. Barik, S.K. Dash and A. Guha,"Experimental and numerical investigation of air entrainment into an infrared suppression device,"*Applied Thermal Engineering*75, pp 33-44, 2015.

[11] S.R. Sahu andD.P. Mishra,"Effect of Pipe Configurations on Air Entrainment into a Louvered Cylindrical Pipe: A Comparison between Open and Close Entrance of a Pipe"*International Journal of Engineering Research* 4, pp 173-177, 2015.
[12] S.R. Sahu andD.P. Mishra,"Maximum air suction into horizontal open ended cylinder louvered pipe,"*Journal of Engineering Science and Technology*, 12(2), pp 388-404, 2017.
[13] S.R. Sahu andD.P. Mishra,"Numerical investigation of maximum air entrainment into cylindrical louvered Pipe,"*International Journal of Automotive and Mechanical Engineering* 13(2), pp 3278-3292, 2016.
[14] C.W. Mohd Noor, R. Mamat, G. Najafi, M.H. Mat Yasin, C.K. Ihsan andM.M. Noor,"Prediction of marine diesel engine performance by using artificial neural network Model"*Journal of Mechanical Engineering and Sciences* 10(1), pp 1917-1930, 2016.
[15] S. K. Dash, "Heatline visualization in turbulent flow." Int. Journal of Numerical Methods for Heat and Fluid Flow, 6(4), pp. 37-46, 1996.